Journal of New Technology and Materials (JNTM)
J. New Technol. Mater.
Vol. 09, N°01 (2019)59-69

OEB Univ. Publish. Co.

The impact of wall emissivity on the thermal and dynamic behavior of an air channel integrated into the roof

Dalila Ababsa

Department of Sciences of Matter, Faculty of Sciences, University of Batna, Algeria

Corresponding author: d_ababsa@hotmail.com

Received date: Dec. 06, 2018 ; revised date: Feb. 20, 2019 ; accepted date: Apr. 24, 2019

Abstract

Because roofs provide a large area to collect solar energy, they can be exploited to arrive at an architectural element that can act as a solar collector and participate in the improvement of thermal comfort. in this axis and in order to show the importance of radiative exchanges in thermosyphon systems and the choice of roofing construction materials; a 3D numerical study is carried out on the natural convection coupled with radiative exchanges in an inclined air channel (using the commercial computational fluid dynamics software FLUENT). Emissivity values tested correspond to those of some building materials. From our results we affirm that the emissivity of the external roofing affects the dynamic and thermal behavior of the channels integrated under the roof. So a good choice of material roofing is recommended in order to getting a maximum air heating by solar radiation.

Keywords: Air conditioning, channel, natural convection, radiative heat transfer, roof solar collectors,

1. Introduction

The addition of a solar heating or cooling system to a dwelling is an attractive solution for the economy and the rational use of energy. Passive techniques are highly recommended as they allow the regulation of environmental conditions using natural means.

Solar architecture exploits and promotes the accumulation of solar heat and uses natural or forced heat circulation of the air, and we can avoid the use of devices of high energy consumption, which can be realized by heating the outside air to raise the temperature of living rooms in winter or the release of hot air by creating a stream of air during the summer.

At the base of the thermosyphon principle a wide variety of systems has been developed to achieve a better exploitation of solar energy, among these systems we can cite for example the Trombe walls, the solar chimney and the solar roofs.

The Trombe wall was used for the first time by Professor F. Trombe and architect J. Michel [1]. Then several researches were realized to improve its performances by proposing to add a blade of air [2], to use a double cover [3] and to integrate protections (curtains) [4]. As well as new configurations have been proposed [5, 6, 7].

According to Guohui Gan [8]; if solar energy is used for passive cooling, the solar chimney is preferable compared to a high wall, so several research works have been done to develop this system [9, 10, 11, 12, and 13], show its effectiveness [14], and improve its performance [8, 15, 16, and 17].

Solar roof ventilation can work better than a Trombe wall in hot climates as it provides a large surface area for collecting solar energy and, as a result, air with higher temperatures [2]. For this, several studies have been carried out with the aim of improving the efficiency of such systems by proposing new configurations [18, 19, 20, 21, and 22]. The addition of radiative barriers can also improve its effectiveness [23].

In hot and humid climates, the small differences in temperature between outside and inside affect the efficiency of solar air conditioning systems. As a result, a new strategy has been proposed [24], which consists of combining a solar roof with a vertical chimney. This system has been studied experimentally and theoretically. According to the results obtained, the authors stated that the system can generate large differences in temperature.

Increasing the heat exchange surface with air without affecting the dimensions of the solar system is one of these improvements, which was the goal of a series of recent numerical studies [25, 26, 27, 28, and 34] and whose objective is the study of the dynamic and thermal behavior of a channel placed under a roof of a building which plays the same role as a solar collector while looking at the effect of the different parameters (the temperature difference and the distance between the two plates, the inclination, the effect of the radiative exchanges between surfaces, etc.) on its efficiency.

According to the literature, radiative exchanges do not attract the attention of researchers; although it has about 30% of total heat exchange in thermosyphon systems (see Table.1). Therefore, we find it useful to conduct this study to show their importance and the importance of the choice of building materials; through studying the walls emissivity effect on the heat exchange in an air channel integrated under roof. So in this paper, we tried to approach the real conditions of a solar roof by studying the effect of the emissivity of materials on the behavior of such a system. The natural convection coupled with the radiative heat transfer is numerically studied using a commercial computational fluid dynamics software (FLUENT), where the governing equations are discretized using the finite volume method, the SIMPLE algorithm is used to couple the speed and the pressure. The geometry is created and meshed by using Gambit 2.2.30. A flow condition has been imposed on the wall which is more realistic; the emissivities tested are those of certain materials used in the construction of roofs.

After a results validation, we have shown the effect of walls radiation on temperature and velocity distribution. After that, we have presented the emissivity effect of roofing materials on Nusselt number and convection coefficient. Through this study, we recommend a good selection of roofing material construction in order to improve the exploitation of solar energy in thermal comfort amelioration.

2. Conception and principle of the studied model

Our general idea is based on the transformation of one of the architectural elements, which is the roof, into a living element by integrating a ventilated air space. This element can contribute to the improvement of the thermal comfort in the rooms by air conditioning in summer and heating in cold period (See fig.1).

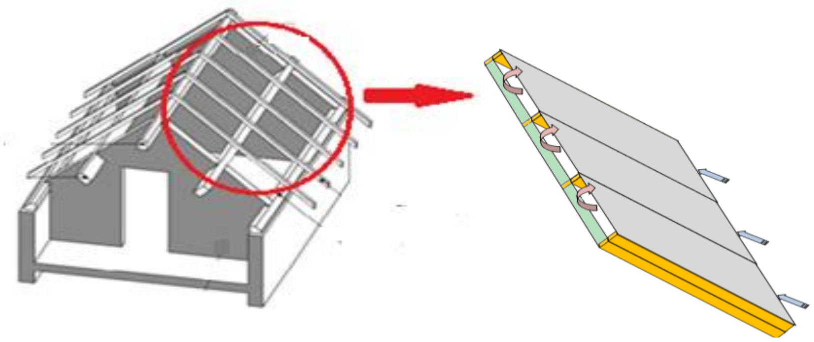

Figure1. Representative 3D diagram of the roof incorporating a ventilated air space.

3. Description of the studied configuration

The physical model studied is an inclined channel of an angle θ, formed by two parallel plates distant from H. of length L = 1.36m and width l = 0.68m.

The channel is traversed by an upward flow of air, entering with ambient temperature (Fig. 2).

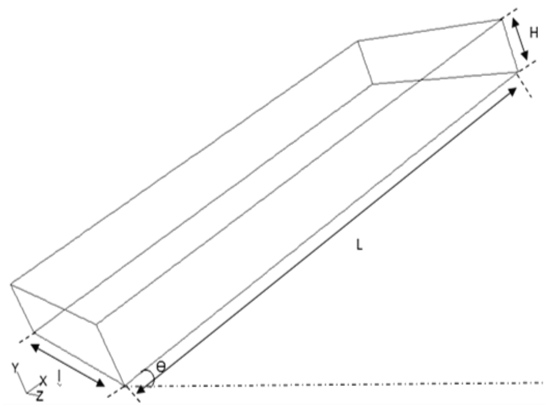

Figure 2. Descriptive diagram of the flat plate channel.

4. Equations governing the phenomenon

As a consequence of the large scales of roof-integrated solar systems, the Rayleigh number is usually $Ra \geq 10^6$, the studied convective flow is transient or completely turbulent [29].

So the equations must be written using Reynolds decomposition. Taking into account simplifying assumptions, the equations governing the problem take the following form:

- Equation of continuity:

$$\frac{\partial \overline{U}_i}{\partial \overline{x}_i} = 0, \qquad i = 1, 2, 3 \tag{1}$$

- Equation momentum

$$\overline{U}_j \frac{\partial \overline{U}_i}{\partial x_j} = -\frac{1}{\rho}\frac{\partial \overline{P}}{\partial x_i} + \frac{\partial}{\partial x_j}\left[(\upsilon + \upsilon_t)\frac{\partial \overline{U}_i}{\partial x_j}\right] + g_i \beta_T (\overline{T} - T_0) \tag{2}$$

Where:

$$\upsilon_t = C_\mu \frac{k^2}{\varepsilon} \tag{3}$$

- Energy equation:

$$\overline{U}_j \frac{\partial \overline{T}}{\partial x_j} = \frac{\partial}{\partial x_j}\left[(\alpha + \alpha_t)\frac{\partial \overline{T}}{\partial x_j}\right] \tag{4}$$

Since the use of the K-ε model gives realistic velocities and temperatures as required by the theory [30], it is chosen as a closure model where K and ε can be calculated by the following equations [31]:

$$\bar{U}_j \frac{\partial k}{\partial x_j} = \frac{\partial}{\partial x_j}\left[\left(\nu + \frac{\nu_t}{\sigma_k}\right)\frac{\partial k}{\partial x_j}\right] + \nu_t \frac{\partial \bar{U}_i}{\partial x_j}\left[\frac{\partial \bar{U}_i}{\partial x_j} + \frac{\partial \bar{U}_j}{\partial x_i}\right] + \frac{\beta}{\rho} g_i \frac{\nu_t}{Pr_t}\frac{\partial \bar{T}}{\partial x_j} - \varepsilon \quad (5)$$

$$\bar{U}_j \frac{\partial \varepsilon}{\partial x_j} = \frac{\partial}{\partial x_j}\left[\left(\nu + \frac{\nu_t}{\sigma_\varepsilon}\right)\frac{\partial \varepsilon}{\partial x_j}\right] + \frac{C_{1\varepsilon}}{\rho}\frac{\varepsilon}{k}\nu_t \frac{\partial \bar{U}_i}{\partial x_j}\left[\frac{\partial \bar{U}_i}{\partial x_j} + \frac{\partial \bar{U}_j}{\partial x_i}\right] + \frac{C_{1\varepsilon}C_{3\varepsilon}}{\rho}\frac{\varepsilon}{k}\left[\frac{\beta}{\rho} g_i \frac{\nu_t}{Pr_t}\frac{\partial \bar{T}}{\partial x_j}\right] - C_{2\varepsilon}\frac{\varepsilon^2}{K} \quad (6)$$

The model constants have the following values [31]:

$C_\mu = 0.09$,

$\sigma_K = 1.0$,

$\sigma_\varepsilon = 1.3$,

$C_{1\varepsilon} = 1.44$,

$C_{2\varepsilon} = 1.92$,

$C_{3\varepsilon} = 1$.

Radiative mechanisms are governed by the radiative transfer equation. It reflects the fact that the local variations of the intensity $I(\vec{r},\vec{s})$ result from a balance between attenuation by absorption and diffusion, and reinforcement by own emission and diffusion in the direction considered from all directions [32].

The Radiative equation is written [31]:

$$\frac{dI(\vec{r},\vec{s})}{ds} + (\alpha + \sigma_s) I(\vec{r},\vec{s}) = \alpha n^2 \frac{\sigma T^4}{\pi} + \frac{\sigma_s}{4\pi}\int_0^{4\pi} I(\vec{r},\vec{s'})\, \emptyset(\vec{s}\cdot\vec{s'})\, d\Omega' \quad (7)$$

5. Boundary conditions

The upper plate is subjected to a constant heat flow while the lower plate is supposed adiabatic as shown in the figure below (Figure 3). The air passing through the channel enters and exits at the pressure and at the ambient temperature. The side walls are adiabatic.

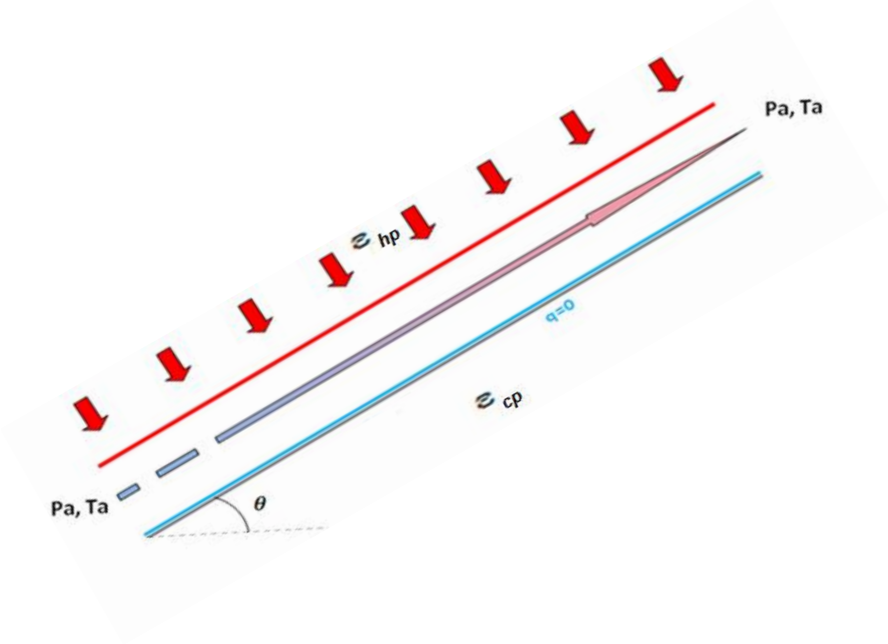

Figure 3. Descriptive diagram of the boundary conditions.

6. Results and discussion

6.1. Validation of results

The comparison between our numerical results and experimental ones of J Khedari et al [26] show that the maximum difference is 7% for the air temperature (fig. 4).

Thus, the radiative model is validated by the numerical work of H.F. Nouanégué and E. Bilgen [28] and the experimental work of Krishnan et al [35]. Table.1 shows a comparison of the ratio between the radiative flux and the total flux (denoted (q_r/q_T)) of this work and the works cited, where q_r is the radiative flux and q_T is the total flux.

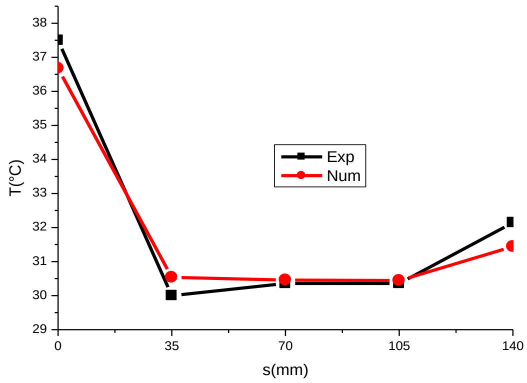

(a) 0.037L.

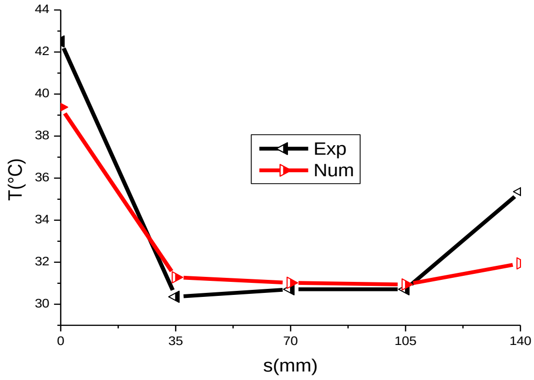

(b) 0.34L

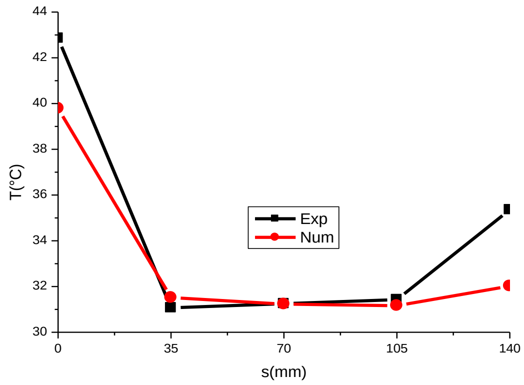

(c) 0.65L.

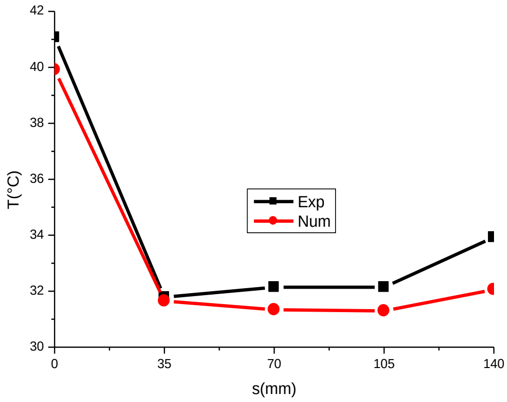

(d) 0.96L

Figure 4. Temperature profiles through the channel for different positions (L is the length of the channel).

Table 1 : Validation of radiatif model

Author	Present work	H.F. Nouanégué et al (2009) [28]	Krishnan et al (2004) [35]
H (m)	q_r/q_T	q_r/q_T	q_r/q_T
0.0175	0.361	0.333	0.347
0.037	0.405	0.439	0.436

6.2. Effects of radiative exchanges on the dynamic and thermal field

In the above, we set the thickness of the channel at the optimum value which is equal to 0.07m [34]. The ambient pressure is taken equal to 1.01325 10^5 Pa. The ambient temperature is 30 ° C.

Fig. 5 represents the effect of radiative exchanges on the thermal field in a longitudinal section where (a) corresponds to a pure convection ($\varepsilon_{hp} = \varepsilon_{cp} = 0$) and (b) corresponds to a natural convection coupled to the radiation ($\varepsilon_{hp} = 0.93$, $\varepsilon_{cp} = 0.90$). According to this figure, it can be seen that the radiative exchanges have an effect on the temperature distribution; this is also affirmed by Ko, Min Seok [33], It is clear that the air layer near the bottom wall is warmer in case of coupled transfer; this is explained by the fact that the lower plate heats up by radiation and transfers this heat to the air passing through the channel (see Fig. 5).

Fig. 6 shows the variation of the temperature along the thickness for three positions taken along the channel. From this figure it is noted that the radiative exchange decreases the maximum temperature of the upper plate from 323.83K to 317.18K on the one hand, and on the other hand it increases the maximum temperature of the lower plate from 305.60 K to about 313.22 K which also allows to heat more air layers located near the bottom plate, it allows us to say that the radiative exchanges can heat the inner face of the roof and that the ventilation of the roof is not only the ideal solution and you have to make a good choice of materials.

Fig. 7 represents the velocity field in a longitudinal section for the two cases, (a) pure convection ($\varepsilon_{hp} = \varepsilon_{cp} = 0$) and (b) convection coupled to the radiative transfer ($\varepsilon_{hp} = 0.93$, $\varepsilon_{cp} = 0.90$). This figure shows that the maximum speeds (of the air zone near the upper plate) decrease under the effect of radiative exchanges (Due to the decrease in temperature differences between the wall and the heated air); however, this speed increases for the rest of the field compared to the case of pure convection.

In fig. 8 we represent the variation of the velocity along the channel for pure convection (a) and convection coupled with radiative exchanges (b). It is noted that close to the channel inlet (section 0.15L), the speed is high in the case of the coupled convection because the radiative exchanges increase the temperature of the lower plate which increases the differences in temperatures between the air and the walls and consequently the buoyancy forces. At the center and at the outlet of the channel (section 0.50L and 1.00L), it is observed that close to the hot wall the velocities decrease in the case of convection coupled with radiation, which is due to the decrease of the temperature differences (responsible for the convective movement) because of the cooling of this wall. Close to the cold wall the radiative exchanges increase the speed which due to the elevation of the differences of the temperatures because of the heating of this last wall.

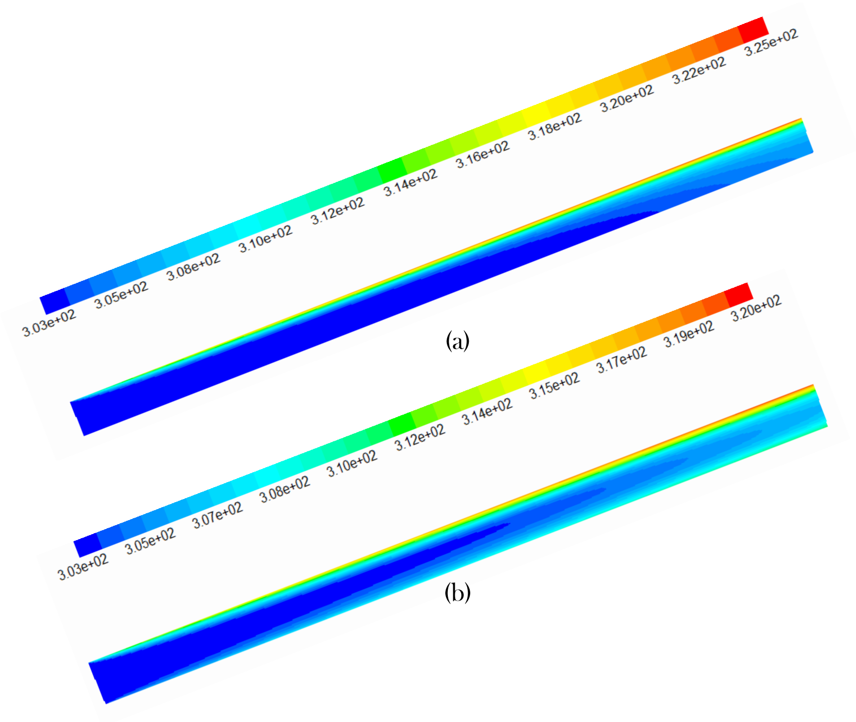

Figure 5. Effect of radiative exchanges on the temperature field, (a) without radiation, (b) with radiation.

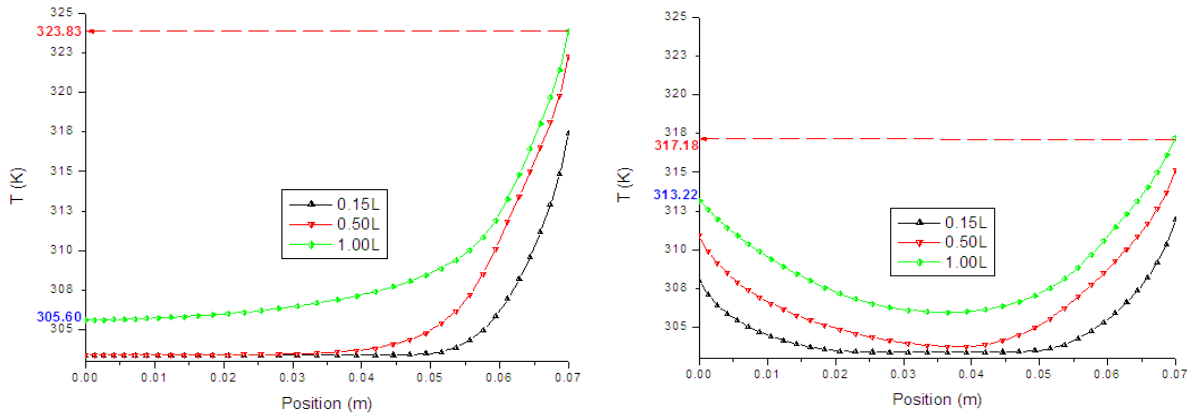

(a) (b)

Figure 6. Effect of radiative exchanges on temperature profiles, (a) without radiation, (b) with radiation.

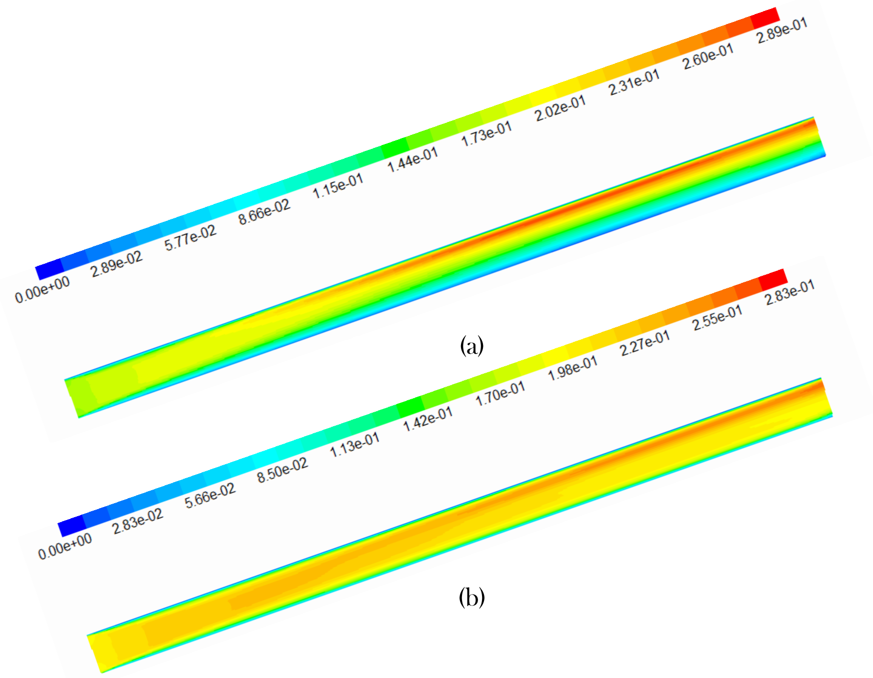

(a)

(b)

Figure 7. Effect of radiative exchanges on velocity field, (a) without radiation, (b) with radiation.

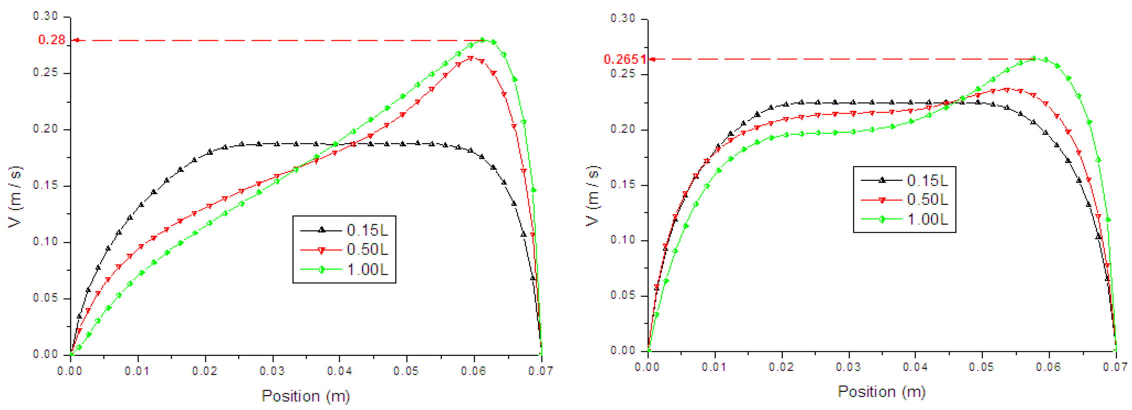

(a) (b)

Figure 8. Effect of radiative exchanges on velocity profiles, (a) without radiation, (b) with radiation.

6.3. Impact of the walls emissivity

Given the importance of the emissivity of materials in radiative exchanges, it was considered useful to test its effect to see how the choice of materials can affect the behavior of such a system. Thus the emissivity of the upper and lower plates was chosen in a way that allows us to get closer to a real roof. Hence we varied the emissivity of the upper plate between 0.02, 0.93, which correspond to those of the polished Zinc and tile, and the emissivity of the lower wall have been varied between 0.25 and 0.90 which correspond respectively to the panel of calcium silicate and white wood. So we tested three cases that are based on the change of materials, these cases are grouped in Table 2.

6.3.1. Effect of emissivity on the exchange coefficient and the Nusselt number.

Fig. 9, Fig. 10 and Fig. 11 represent the exchange coefficient (a) and the number of Nusselt on the upper plate (b) for tests 1, 2, and 3, respectively.

For test 1, we notice that; for higher emissivity top plates the increase of the emissivity of the lower plate (by fixing that of the upper plate) increases the exchange coefficient and consequently the Nusselt number of the upper plate (see Fig. 9). This is because when the upper plate is of high emissivity it provides a significant radiative energy to the lower plate, the latter heats up which allows it to release a quantity of radiative heat, which allows heating the upper plate hence the increase of the exchange coefficient.

Table 2: *Tested cases*

tested case	Upper plate		Bottom plate	
	materials	emissivity ε_{hp}	materials	emissivity ε_{cp}
1	Tile	0.93	Calcium silicate panels	0.25
	Tile	0.93	White wood	0.90
2	Polished zinc	0.02	White wood	0.90
	Tile	0.93	White wood	0.90
3	Polished zinc	0.02	Calcium silicate panels	0.25
	Polished zinc	0.02	White wood	0.90

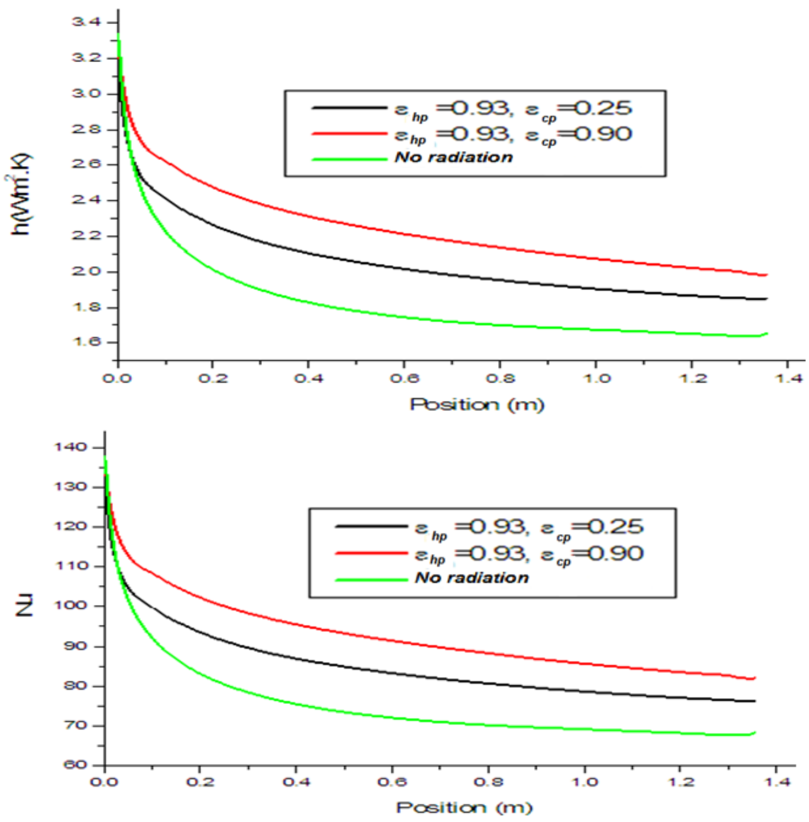

(a)

(b)

Figure 9. Effect of wall emissivity on the exchange coefficient (a) and the local Nusselt number of the upper wall (b), case of test 1.

The test 2 shows us that for low emissivity of the upper plate the exchange coefficient and the Nusselt number keep values close to those of the case of pure convection even if the emissivity of the lower plate is high. So we can say that the emissivity of the upper plate has a significant effect in radiative exchanges (see fig.10).

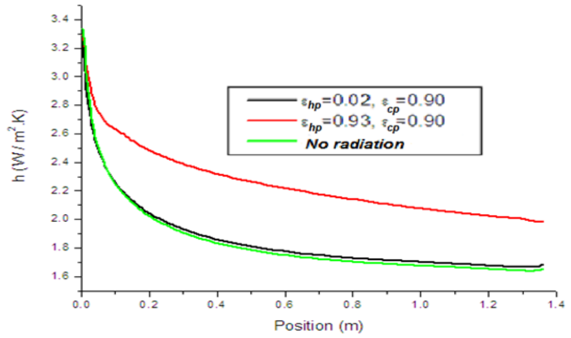

(a)

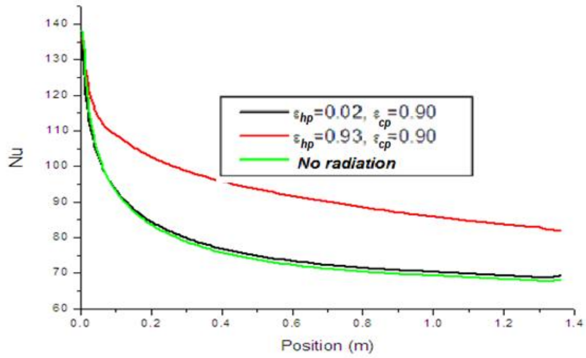

(b)

Figure 10. Effect of wall emissivity on the exchange coefficient (a) and the local Nusselt number of the upper wall (b), case of test 2.

Fig. 11 shows the effect of the emissivity of the walls of the heat transfer coefficient (a) and the local Nusselt number of the upper wall (b) in the case of test 3, here it is confirmed that in the case of a low emissivity of the upper plate (regardless of the emissivity of the lower plate) the exchange coefficient and the Nusselt number are not affected by the radiative exchanges, which allows us to say that the upper plate is still the major supplier of heat in the form of convective or radiative exchange.

6.3.2. Effect of emissivity on temperature profiles

Fig. 12 represents the effect of emissivity on the temperature profiles.

The effect of the emissivity of the bottom plate appears for large emissivity of the top plate, where the radiative heat exchange cools the upper heat plate and the bottom plate. But for low emissivity of the latter, the effect of the emissivity of the lower plate becomes negligible which gives the importance of the materials of the outer cover of the roof.

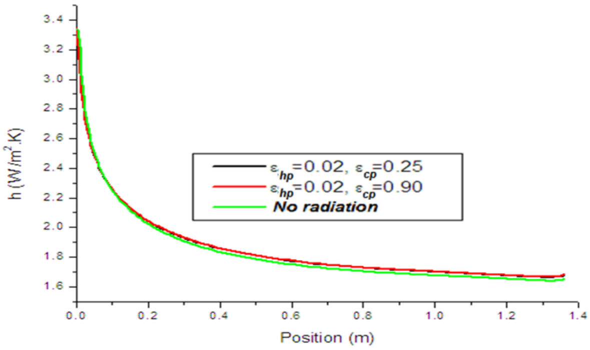

(a)

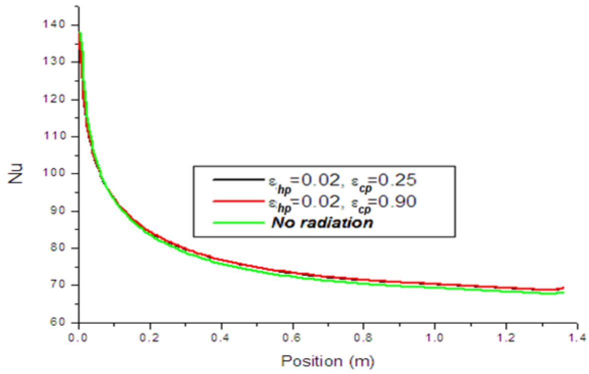

(b)

Figure 11. Effect of wall emissivity on the exchange coefficient (a) and the local Nusselt number of the upper wall (b), case of test 3.

6.3.3. Effect of emissivity on velocity profiles

The dynamic field is also affected by the emissivity of the canal walls (Fig. 13). It is very clear that for a low emissivity of the upper plate the velocity profiles are no longer affected even if the lower plate is of high emissivity, but when the upper plate is of high emissivity we can see the effect of the emissivity of the lower one. So we can say that the emissivity of the outer covering of the roof affects the dynamic thermal behavior of integrated channels under roof, and its effect is significant compared to the emissivity of the bottom plate.

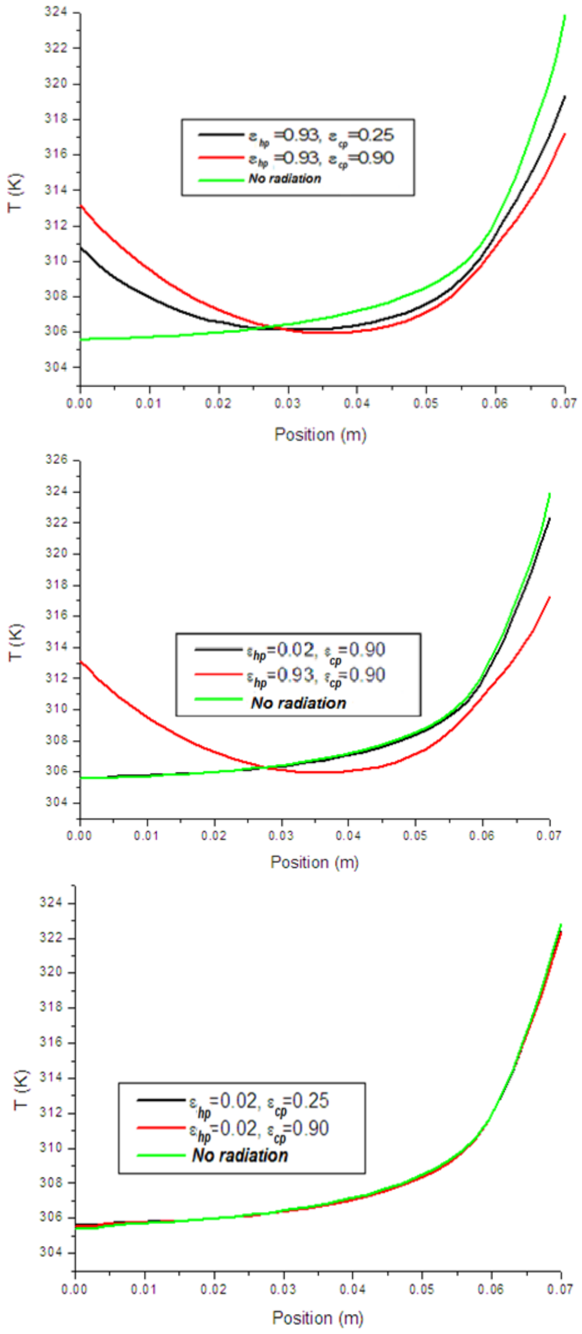

Figure 12. Effect of emissivity on temperature profiles.

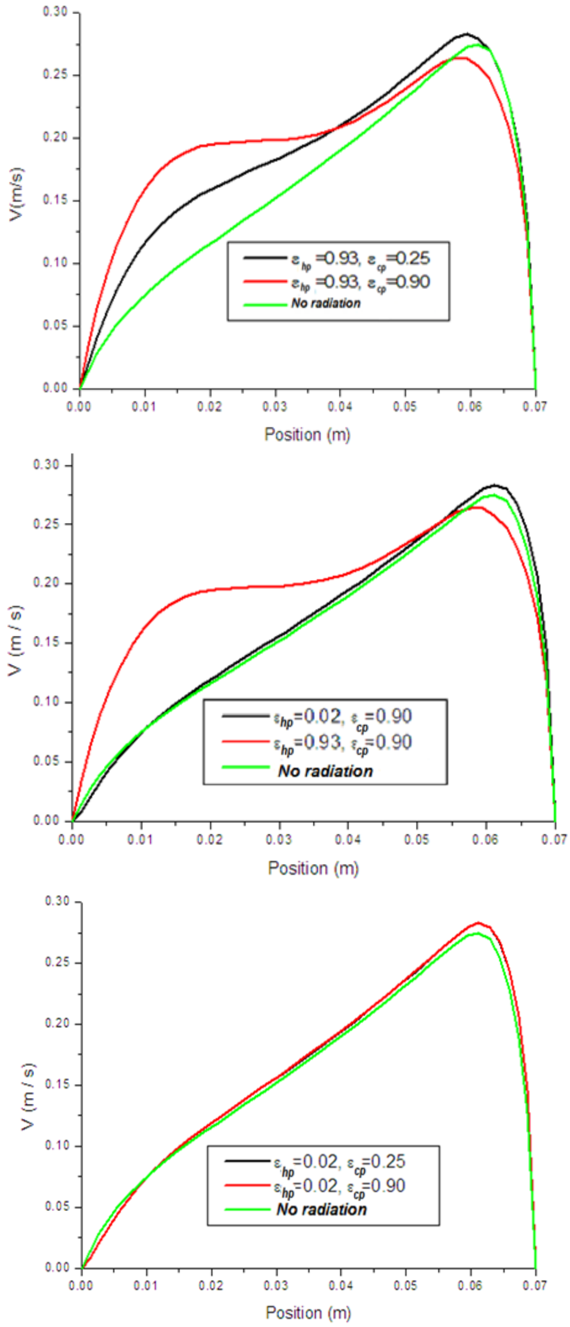

Figure 13. Effect of emissivity on speed profiles.

7. Conclusion

Natural convection with radiative exchange has been studied in an attic channel. A series of validation tests was carried out. These validation tests were carried out on a flat plate channel experimentally studied by J. Khedari et al [26], the numerical results obtained are in good agreement with those obtained by this author. The results of the radiative model were validated by those of H.F. Nouanégué et al (2009) [28]. In this paper we have tested the effect of the choice of materials through their emissivity. From the results obtained, the following conclusions were drawn.

- Radiative exchanges between surfaces have a significant effect, so this must be taken into account in heat transfer studies.
- The thermal and dynamic behavior is affected considerably by the radiative exchanges and the emissivity of the walls
- In numerical simulation, thermal boundary conditions have a considerable effect on the analysis of the effect of radiative exchanges, so realistic boundary conditions must be chosen.

- The emissivity of the upper plate has a dominant effect on the convection coefficient and the Nusselt number compared to that of the lower plate.

- The emissivity of the roof's outer cover affects the dynamic and thermal behavior of the roof-integrated channels, and its effect is significant compared to the emissivity of the lower plate.

Nomenclature

Symbols

α	Thermal diffusivity, $m^2.s^{-1}$
l	Channel width, m
L	Channel length, m
C_p	Heat capacity, J. $kg^{-1}.K^{-1}$
H	Channel thickness, m
g	Gravity acceleration, m. s^{-2}
k	Turbulent kinetic energy, m^2. s^{-2}
ε	Dissipation, $m^2.s^{-3}$
P	Pressure, Pa
q	Heat flux, W
T	Temperature, °C, K
I	Radiative intensity
U	X velocity, m. s^{-1}
V	Y velocity, m. s^{-1}
W	Z velocity, m. s^{-1}
x, y, z	Cartesian coordinates
$\vec{r}$	Vector position
$\vec{s}$	Direction vector
$\vec{s'}$	Vector direction of dispersion
α	Absorption coefficient
n	Refractive index
σ_s	Coefficient of dispersion
$\emptyset$	Phase function
$\acute{\Omega}$	Solid angle

Greek letters

β_T	Coefficient of thermal expansion isobaric , K^{-1}
μ	Dynamic viscosity, Pa. s^{-1}
ν	Kinematic viscosity, m^2. s^{-1}
ρ	Density, kg. m^{-3}
ρ_0	Density at reference temperature T_∞ kg. m^{-3}
ε	Thermal emissivity
θ	Tilt Angle, (°)
σ	Constant of Stefan-Boltzmann, W. $m^{-2}.K^{-4}$

Dimensionless numbers

Pr	Prandtl number
Ra	Rayleigh number

Indices

a	atmospheric
$_0$	Reference
L	Based on the channel length
t	turbulent
T	Based on temperature
r	radiative
hp	hot plate
cp	cold plate
i, j	index concept coordinates

References

[1] K. Imessad, "Le chauffage Solaire Passif dans l'Habitat", Bulletin des Energies Renouvelables. N°4 Decembre 2003.

[2] Chan, Hoy-Yen, B. Saffa Riffat and Jie Zhu, "Review of passive solar heating and cooling technologies." Renewable and Sustainable Energy Reviews 14, 2 (2010) 781-789.

[3] Gan, Guohui, "A parametric study of Trombe walls for passive cooling of buildings" Energy and buildings 27,1 (1998) 37-43.

[4] B. Chen, X. Chen, Y. H. Ding, and X. Jia, "Shading effects on the winter thermal performance of the Trombe wall air gap: An experimental study in Dalian." Renewable Energy 31, 12 (2006) 1961-1971.

[5] J. Hirunlabh, W. Kongduang, P. Namprakai, and J. Khedari, "Study of natural ventilation of houses by a metallic solar wall under tropical climate." RenewableEnergy, 18, 1 (1999) 109-119.

[6] L. Zalewski, S. Lassue, B. Duthoit and M. Butez, "Study of solar walls—validating a simulation model." Building and Environment 37, 1 (2002) 109-121.

[7] Chen Wei and Wei Liu, "Numerical analysis of heat transfer in a composite wall solar-collector system with a porous absorber" Applied Energy 78, 2 (2004) 137-149.

[8] Gan Guohui, "Simulation of buoyancy-induced flow in open cavities for natural ventilation." Energy and buildings 38,5 (2006) 410-420.

[9] P. Raman, Sanjay Mande, and V. V. N. Kishore "A passive solar system for thermal comfort conditioning of buildings in composite climates." Solar Energy 70, 4 (2001) 319-329.

[10] K. S. Ong, "A mathematical model of a solar chimney" Renewable energy 28, 7 (2003) 1047-1060.

[11] K. S Ong and C. C. Chow, "Performance of a solar chimney." Solar energy 74, 1 (2003) 1-17.

[12] Lee Kwang Ho, and K. Strand Richard "Enhancement of natural ventilation in buildings using a thermal chimney." Energy and Buildings 41, 6 (2009) 615-621.

[13] Wei Du, Yang Qirong, and Zhang Jincui "A study of the ventilation performance of a series

of connected solar chimneys integrated with building" Renewable energy 36, 1 (2011) 265-271.

[14] T. Miyazaki, A. Akisawa, and T. Kashiwagi, "The effects of solar chimneys on thermal load mitigation of office buildings under the Japanese climate" Renewable Energy 31.7: (2006) 987-1010.

[15] D. J. Harris, and N. Helwig, "Solar chimney and building ventilation", Applied Energy 84, 2 (2007) 135-146.

[16] Bassiouny Ramadan, and Nader SA Koura, "An analytical and numerical study of solar chimney use for room natural ventilation." Energy and buildings 40, 5 (2008) 865-873.

[17] E. P. Sakonidou, T. D. Karapantsios, A. I. Balouktsis, and D. Chassapis, "Modeling of the optimum tilt of a solar chimney for maximum air flow." Solar Energy 82, 1 (2008) 80-94.

[18] Joseph Khedari, Weerapong Mansirisub, Sompong Chaima, Naris Pratinthong, Jongjit Hirunlabh, "Field measurements of performance of roof solar collector." Energy and Buildings 31, 3 (2000) 171-178.

[19] J. Hirunlabh, S. Wachirapuwadon, N. Pratinthong, and J. Khedari, "New configurations of a roof solar collector maximizing natural ventilation", Building and Environment 36, 3 (2001) 383-391.

[20] J. Waewsak, J. Hirunlabh, J. Khedari, and U. C. Shin, "Performance evaluation of the BSRC multi-purpose bio-climatic roof", Building and Environment 38, 11 (2003) 1297-1302.

[21] X. Q. Zhai, Y. J. Dai, and R. Z. Wang, "Comparison of heating and natural ventilation in a solar house induced by two roof solar collectors", Applied Thermal Engineering 25, 5-6 (2005) 741-757.

[22] Chang Pei-Chi, Che-Ming Chiang, and Chi-Ming Lai, "Development and preliminary evaluation of double roof prototypes incorporating RBS (radiant barrier system)." Energy and Buildings 40, 2 (2008) 140-147.

[23] Lai Chi-ming, J. Y. Huang and Jenq-Shing Chiou, "Optimal spacing for double-skin roofs." Building and Environment 43, 10 (2008) 1749-1754.

[24] Wardah Fatimah Mohammad Yusoff, Elias Salleh, Nor Mariah Adam, Abdul Razak Sapian, Mohamad Yusof Sulaiman, "Enhancement of stack ventilation in hot and humid climate using a combination of roof solar collector and vertical stack", Building and Environment, 45, (2010) 2296-2308.

[25] D. Ababsa and S. Bougoul. "Numerical Study of Natural Ventilation Through a Roof Cavity for Reduction of Solar Heat Gain", Energy Procedia 18 (2012) 974-982.

[26] Dalila Ababsa, and Saadi Bougoul, "Numerical study of natural ventilation in a channel integrated below the roof tiles of Buildings", International Journal of Innovation and Applied Studies 5, 3 (2014) 222-232.

[27] Dalila Ababsa, and Saadi Bougoul. "Numerical Analysis of Thermal and Dynamic Behavior of a Roof Solar Collector", Heat Transfer—Asian Research 46, 5 (2017) 447-464.

[28] Dalila Ababsa, Saadi Bougoul, "Modeling of natural convection and radiative heat transfer in inclined thermosyphon system installed in the roof of a building", Heat Transfer—Asian Res. (2017) 1–10, Doi: 10.1002/htj.21266.

[29] B. Zamora and A. S. Kaiser, "Optimum wall-to-wall spacing in solar chimney shaped channels in natural convection by numerical investigation" Applied Thermal Engineering 29, 4 (2009) 762-769.

[30] E. Bacharoudis, M. G. Vrachopoulos, M. K. Koukou, D. Margaris, A. E. Filios, and S. A. Mavrommatis, "Study of the natural convection phenomena inside a wall solar chimney with one wall adiabatic and one wall under a heat flux." Applied Thermal Engineering 27, 13 (2007) 2266-2275.

[31] Fluent Inc, Fluent 6.3 User's Guide, (2005).

[32] El Kasmi, Amina, "Application de la méthode des ordonnées discrètes au transfert radiatif dans des géométries bidimensionnelles complexes: couplage rayonnement-convection", Mémoire de maîtrise, Université du Québec à Chicoutimi, 1999.

[33] Min Seok Ko, "Numerical simulation of three-dimensional combined convective radiative heat transfer in rectangular channels," Ph.D., Department of Mechanical Engineering, Texas A & M University Dec 2007

[34] D. Ababsa, Doctorate Thesis, 2016, University of Batna 1, Algeria

[35] A. S. Krishnan, B. Premachandran, Chakravarthy Balaji, S. P. Venkateshan "Combined experimental and numerical approaches to multi-mode heat transfer between vertical parallel plates." Exp Therm Fluid Sci 29, 1 (2004) 75-86.